The Thesis Committee for Sahil Shanghavi
Certifies that this is the approved version of the following thesis:

Feasibility Study of an Integrated Wind and Solar Farm by Evaluating the Wind Turbine Shadows

APPROVED BY
SUPERVISING COMMITTEE:

Supervisor:

W. Mack Grady

Surya Santoso

Feasibility Study of an Integrated Wind and Solar Farm by Evaluating the Wind Turbine Shadows

by

Sahil Shanghavi, BS

Thesis

Presented to the Faculty of the Graduate School of

The University of Texas at Austin

in Partial Fulfillment

of the Requirements

for the Degree of

MASTER OF SCIENCE IN ENGINEERING

The University of Texas at Austin

May 2012

Dedication

I would like to dedicate this thesis to my family, friends, teachers and well-wishers – the people without whom I would not have been able to reach the point leading up to this thesis. First and foremost, it is dedicated to my Godfather, Ravi Todi, who by example taught me to work as hard as possible, without worrying about the rewards that could follow. He helped me understand that being positive and patient always leads to good things, even though the path might be filled with difficulties. To my Godmother, Sarika Todi, who demonstrated that as long as we set our priorities right, no matter how hard a situation we might be faced with, all challenges can be overcome. To my parents, Leena and Ketan Shanghavi, who have had the biggest influence on the most important decisions I have taken in my life. Thanks to them even after being away from all of my family in India, since 6 years, I still feel like I am home as they have made it a point to speak with me at least once a day. Without their love and support I would not have survived even one day living so far away from them, and the rest of my family.

It is dedicated to all my family members without whom I would be incomplete. My grandparents, Taraben and Mandaldas Shanghavi, Rekha and Anil Chhajer, and my great grandmother – 'Maa', Ava Kumari Nahar, through their pride in me, have given me more motivation and reasons to excel than I ever thought possible. Due to my family's faith and confidence in me, I have been able to push myself harder and give in a 110% to all my endeavors. This thesis is also dedicated to all the members of my UMass family. They gave me all their love and affection, even though I was just a regular student.

Lastly, this thesis is dedicated to my beloved sister, Akriti Shanghavi, who has always sacrificed herself to enable me to get the best opportunities. Her belief in me, and her constant adulation has helped pick me up whenever I have hit a low point in my life.

Acknowledgements

This thesis could not have been completed without the whole-hearted help from Dr. W. Mack Grady. His insights, support and regular feedback cannot be emphasized enough. He helped me nurture an innocent idea into a full-blown research topic and a thesis. Without the time and effort he put into advising me, this thesis could not have even been started. I would like to thank him for all his patience with me. The contributions in my education, from one of my best friends, Shanka Wijesundara, have been immeasurable. He has been my pillar of support for the last 4 years, and during my time in graduate school he has listened to me and helped me chose the path I have taken. He has also been a great asset to bounce ideas off of. Even when I started out learning Matlab, he was the expert who guided me whenever I needed some direction.

It must be acknowledged that I probably would not have ever pursued a graduate degree in engineering, had I not received the best and most meaningful advise from Dr. Theodore Djaferis and Dr. Christopher Hollot at UMass Amherst. I would also like to acknowledge the contributions of the Professors from the University of Massachusetts Amherst and from the University of Texas at Austin for providing me with the knowledge required to reach this level. I would also like to thank the staff from both these universities for making things easier for me, and for constantly helping me out with all the necessary paperwork. I would like to especially thank Melanie Gulick, as the support and guidance I received from her helped me stay positive throughout my time in graduate school. As my job supervisor, she was very flexible with me and allowed me ample time to work on this thesis, as was necessary.

My friends from both the University of Texas at Austin and the University of Massachusetts at Amherst were critical in helping me through the toughest of times I

faced. I would not have been able to complete my thesis without the help provided by my friends Urszula Bosco, Andrea Cataldo, Anamika Dubey, Joel Garcia, Chris Landry, Karan Mendiratta, Warda Razaq, Gurtej Singh Saini, Aparajita Sant, Amir Toliyat, and Shanka Wijesundara. My family and friends from India who were not present with me physically, provided me with the moral support for which I extend my gratitude to Nikhil Almal, Archit Ghuwalewala, Saloni Kaushik, and Ritwick Saharia.

I would also like to thank Austin Energy for graciously providing me with the necessary Solar Data that was used in this thesis. Bradley Schwarz of E.ON Climate and Renewables North America, and Roy Blackshear, manager of the AEP Desert Sky Wind Farm, have also been great supporters of the idea presented in this thesis. They provided essential guidance and feedback.

May 2012

Abstract

Feasibility Study of an Integrated Wind and Solar Farm by Evaluating the Wind Turbine Shadows

Sahil Shanghavi, MSE

The University of Texas at Austin, 2012

Supervisor: W. Mack Grady

This thesis analyzes the feasibility of having an integrated wind and solar farm to optimize the use of land resources and capital investment by evaluating the effect that wind turbine shadows have on the area surrounding them. Two methods are used to predict shadow impact. The first method is based on the traditional textbook "Clear Sky" equations, which have maximum sensitivity to shadows because the method considers every day to be a perfect day. The second method uses measured global-horizontal and diffuse-horizontal solar radiation in units of W/m^2, which take into account the true variations of daily conditions. The calculations are performed for 1 square meter surfaces, over different assumed areas of a wind power plant, for every second of the day. For purposes of shadow calculations, the tip-top height (i.e., tower height plus blade length) is used. All calculations are performed with the specifications of a GE 1.5 MW wind turbine, which is the most commonly used wind turbine in USA.

Table of Contents

List of Figures

List of Equation Steps

Chapter 1

Preface

The global energy requirements have constantly been on the rise, and with technological advances the energy consumption per capita is also rapidly increasing. While there is this increase in the demand for energy, there has also been a tremendous increase in global population. We recently hit a global population of 7 billion people. With a scarcity of resources and rising prices of all commodities, we will have to optimize our use of technology and land, so as to sustain our growth.

Currently the trend with setting up solar or wind power plants is to set them up exclusively. Even so, the number of such power plants is few. This is mainly due to the extremely high initial capital investment. One day while taking one of Dr. Grady's classes on Renewable Energy in my first year, I thought that there might be a simple solution to reducing this high initial capital investment and cost of electricity. This could be done by optimizing the resources we already have, i.e. finding a way to setup the wind and solar power plants on the same land area as they are both extremely land resource intensive when setup up exclusively. This thesis outlines the feasibility of this simple idea by two different methods of measuring the overall daily solar harvest in kWh. This is done by checking the harvest for different areas of a wind power plant, keeping in mind the shading effect from the wind turbines. It also gives a brief overview of what its advantages are over the current methods of exclusive setups focused only on one type of renewable energy, whether it maybe solar or wind.

Chapter 2

Introduction

Benjamin Franklin discovered electricity in 1752, and Thomas Edison created the first ever long lasting artificial light source in 1879. Even then according to the International Energy Agency, after 132 years since the discovery and use of electricity, 1.5 billion people worldwide have no access to it. What is even worse is that in this day and age of heightened technological use, 2.5 billion people subsist completely on traditional fuel sources like wood and charcoal[5].

Even with the existence of this gaping hole between the demand and supply, the global energy demand, from those who have access to it, has been growing at quite a rapid pace. When the issue of climate change and global warming is added to this mix, it poses a serious challenge to the growth of new power generation. As has been known since decades, coal-fired power plants are the easiest and cheapest solution to setup and run for generating electricity. But with policies coming in to curb emissions and improve operating efficiencies of power plants, such as the Cross-State Air Pollution Rule implemented by the Environmental Protection Agency in the USA, renewable energy technologies are slowly becoming more feasible. More importantly renewable energy technologies such as solar and wind have zero emissions which not only help with the climate change and global warming issues, but are also very popular with the groups advocating for use of these technologies to reduce emissions for the same reasons. Additionally, wind and solar energy do not have a fuel cost.

To manage the scope of this thesis effectively, we will see the situation in the United States of America and see how it can be scaled up to the global level. Currently, the United States of America has installed capacities of 603 MW of solar energy and

33,542 MW of wind energy[12]. Globally, these values are 23,000 MW of solar energy and 159,000 MW of wind energy[9]. Thus, USA makes up 21% of the world's total wind energy installed capacity, but only 2.6% of the global solar installed capacity. There are many reasons behind the deployment gap between the solar and wind energy technologies. One of the main reasons is the high cost for solar electricity production, which is estimated to be 22¢ per kWh, whereas the cost of wind electricity production is only 8¢ per kWh[8]. Thus, an implementation needs to be figured out to better utilize available resources to reduce the cost of solar energy production. I believe that utilizing wind and solar energy together on the same site might help bring down a big part of the initial investment that is required when setting up each of these technologies separately.

As the need to fulfill the world's hunger for more energy increases and action is taken globally to reduce our footprint on this planet, solar and wind energy will become extremely essential in the pool of generation technologies to be used.

In this thesis, I use the shadows cast from wind turbines to calculate the change in overall solar kWh harvest available per meter square of area, for any given plot of land within a wind power plant. To analyze the feasibility of setting up wind and solar power on the same land area, it is important to see how much land area can truly be used after seeing the shading effects of the wind turbines. We use different methods and implementations to calculate the overall shading effect from the wind turbines, which can be seen in Chapter 4.

Chapter 3

Wind and Solar Power

3.1 The Potential of Wind and Solar Power

In 2010, the USA had a peak energy demand of 747,836 MW or 748 GW[2]. From the data presented in Figure 1 below, it is clear that maximizing the use of these two technologies can easily fulfill USA's total energy requirements. But, it would not be a feasible choice to only use these technologies, as wind and solar potential are highly variable and not very predictable. Even so, it may be used at a much larger scale than is being currently employed in the USA.

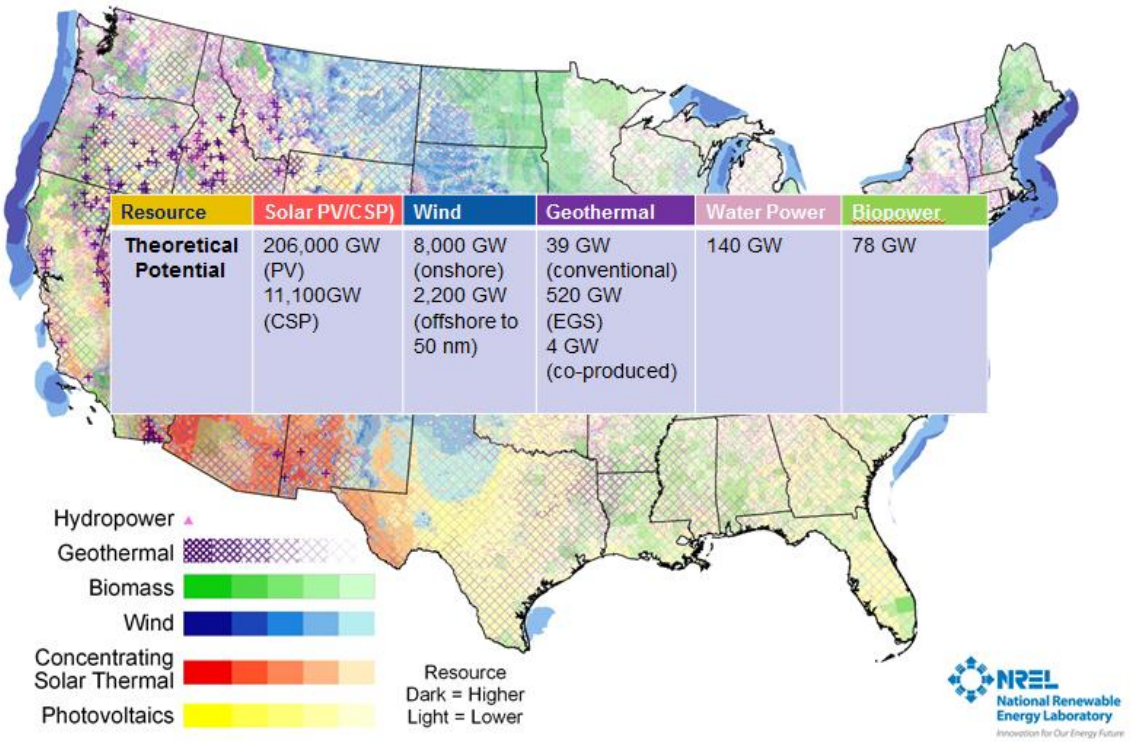

Figure 1 – The figure shows the total theoretical potential of different renewable energy technologies in USA[10]

At the moment, five of the largest wind power projects in the US are all based in Texas. The largest of these is in Roscoe, with a capacity of 782 MW[1]. In section 3.2, I

will explain how the large wind power plants are unable to optimize the potential of the land and the electrical equipment that they use. When we compare the two figures, Figures A1 and A2 in the Appendix that show the solar and wind potential of USA, we see that central USA has excellent solar and wind potential, although the potential of both these technologies are pretty good throughout the country. This potential can be very well utilized and tapped by setting up integrated wind and solar power plants. Even though this seems like a very simple idea, it has not been used much due to the lack of investment and research in the area.

Figure 2 – A picture showing the joint use of wind and solar technologies at the Wild Horse Wind and Solar Facility in Washington[3]

The only instance in the USA where an integrated solar and wind power plant currently exists is located on Whiskey Dick Mountain in Washington, shown in Figure 2. This facility, known as the Wild Horse Wind and Solar Facility, is owned by Puget Sound Energy. It has 149 wind turbines producing 273 MW and 2723 PV's producing

only 0.5 MW[3]. At this rate of use, just looking at Figure 2 and the overall output rating of each generation technology, it seems like they are not able to fully utilize the solar and land potential available to them. Looking at the figure it seems like a lot of land that could be used to setup solar panels has been left barren. To understand this aspect it is important to see how the land is utilized in wind power plants. This is explained in the following section.

3.2 WIND POWER PLANT FOOTPRINT

Figure 3 – Zoomed out satellite image of a wind power plant South of Sweetwater, TX obtained using Google maps

The figure shown above has a shaded blue area that was created using the tools provided by Google maps to get a sense of the amount of land required for setting up a large scale wind power plant. The shaded region contains 85 wind turbines, each of which is represented using the blue place-marks. The total area of the shaded region was calculated to be 10.29 square miles. If we assume the power plant to be employing using GE 1.5 MW which are the most commonly used wind turbines in USA, we would get an installed capacity of 127.5 MW from 85 turbines for a 10.29 square mile area. This would give us an installed capacity of 12.4 MW per square mile, which seems to be a very small number.

Figure 4 – Zoomed in satellite image of a wind plant from the shaded region obtained using Google maps for one square mile area, where the red lines indicate 1 mile

The above image is a zoomed in view showing 11 wind turbines within the 1 square mile area (Note – We assume 12 wind turbines in this area for sake of calculations as there seems to be an empty spot. One of the wind turbine's is assumed to be placed between the leftmost bottom turbine and the vertical red line for optimized calculations). Now, since we assumed the turbines to be GE 1.5 MW turbines we know the length of its blades to be 40 m (0.0248 miles). Hence, if we now assume the 12 turbines to be packed in as close as possible vertically (a little more than twice the blade length), assuming 100 m (0.0621 miles), but spread out horizontally as shown above, the turbines require only 0.0621 square miles. Thus, 93.79% of the effective land area is not utilized and empty.

3.3 ADVANTAGES OF INTEGRATION OF WIND AND SOLAR TECHNOLOGIES

As mentioned in the earlier section, with a purely wind oriented power plant approximately 93.79% of the land area is left unused or wasted, with respect to electricity generation. To optimize the use of this land and the electrical equipment already being used by the wind facility such as transformers, relays, circuit breakers and transmission lines it would make most sense to also setup solar panels in conjunction with the wind turbines. In most places in the USA, wind potential is at its maximum during the night whereas the solar potential is always at its maximum during the day[6]. Hence, as all the electrical equipment is setup for maximum capacity output based on the installed wind capacity, the same infrastructure could easily be utilized for the solar panels. The equipment would be able to provide the necessary capabilities to the wind turbines when they are peaking at night and also to the solar panels peaking during the day. In case there is ever a situation where the wind gusts pick up during the day due to cold or warm fronts, the blades of the wind turbine can be easily pitched to an angle where the blades stop rotating, and thus stop producing electricity to safeguard the electrical equipment from overheating or getting damaged.

To get an estimate of how much energy we can get, by utilizing the space left unoccupied by the wind turbines in one square mile of area, we use the assumption that 1 MW of installed solar panel capacity requires 0.00374 square miles[11]. Thus, for the 0.9379 square miles of area that was left unused by the wind power plant, using a simple calculation we get, $\frac{(0.9379 \text{ square miles})}{(0.00374 \text{ (square miles)/MW})} @ 250 \text{ MW}$, i.e. 250 MW of solar installed

capacity that can be added to the 1 square mile. Although, this is a very big number, due to the distribution of the wind turbines and their shading effects this number would reduce significantly. But even if we consider that we are able to utilize only 5% of that land area to install solar panels, we would still be able to get 12.5 MW of solar installed capacity per square mile of area. This would effectively increase the installed capacity by 70% per square mile from 18 MW only for a wind power plant, to 30.5 MW for an integrated solar and wind power plant.

Thus, the overall advantages of having both wind turbines and solar panels integrated in one power plant are as follows: -

1. The usage of land and other infrastructure, such as electrical equipment, is optimized, which helps bring down the cost of electricity.
2. The overall installed capacity and output from the power plant can be increased significantly. As shown from the calculations earlier it can quite easily be doubled.
3. By the diversification of the types of energy generation used, the variability in the generation is reduced significantly. On cloudy days you may still have lots of wind and on calm days with no wind you may have a lot of strong sunshine.
4. Initial capital investment is significantly reduced by the optimization of the use solar and wind in parallel.
5. The reliability of power coming from such a power plant is also higher than that from only a solar or only a wind power plant. This again is related to the reduction in variability.

Chapter 4

Methodology

4.1 ASSUMPTIONS

In this thesis a typical layout for a West Texas wind farm is assumed. This assumption is based on the fact that Texas has the five largest wind power plants in USA. Furthermore, West Texas is also known to have a lot of economically viable land resource. Also, due to the availability of recent actual solar data measurements, Saragosa, TX is chosen to be the study area for this thesis. West Texas wind farms usually have at least 100 turbines, in a rectangular grid pattern on flat ground, but sometimes in a more complex pattern dictated by the geographical boundaries of a mesa top. The actual plot of land for each wind turbine is approximately 1 km in the prevailing wind direction, by 0.3 km width, yielding an area of 0.3 square km, as can be seen in the appendix in Figure A3. These are the usual values used in conjunction with a GE 1.5 MW wind turbine. Since we use Saragosa as our location, we assume the local longitude to be 103.66°, longitude time zone to be 90.00°, local latitude to be 31.02°. The panel azimuth is taken to be 180° (facing south), and panel tilt to be 30°, which is the most optimum value for having a fixed-tilt throughout the year based on the latitude. The tower tip-top height, which is the maximum height from the base of the turbine to the tip of the blade, is assumed to be 120 m, and the wind turbine maintenance pad is estimated to have a 100 m diameter. In order to account for the annual variation in the weather, when the position of the sun in the sky and the total number of daylight hours change, we simulate four sample weeks to cover all scenarios. The four weeks simulated are the following four time periods: spring and fall equinoxes, and summer and winter solstices. These together account for all seasonal variations during the year.

In our simulations we consider differently sized areas depending on the number of turbines being simulated. We make sure to account for the 0.3 km^2 required plot of land for each turbine. For our simulated areas, we take readings for each square meter box. This gives us a grid pattern of X by Y boxes, where X and Y depend on the number of turbines under consideration, each of 1 m^2 area within the region of interest. The reason we use a 1 m^2 box is because we can easily assume each of these boxes to contain a 1 kW rated solar panel of area exactly equal to 1 m^2. One important point to note is that we consider only the shadows that are outside the turbine maintenance pad having 100 m diameter and within the plot area of interest.

Next, two different methods are used to simulate and obtain the readings of total solar harvest for each of these 1 m^2 boxes. The first method is based on traditional textbook "Clear Sky" equations[4], which have maximum sensitivity to shadows because every day is considered to be a perfect day. The second method uses measured global-horizontal and diffuse-horizontal solar radiation in units of W/m^2, which accounts for the actual variations in the daily weather condition[13]. The calculations for both these methods are performed for 1 square meter surfaces, over the given area, for every second of the day. These are described in the next sections.

4.2 METHOD 1. PREDICTED IMPACT USING CLEAR SKY EQUATIONS

Turbine shadows have the most impact on a surrounding PV array on clear days because the beam of the sun is strongest. This creates a bigger difference in the solar harvest for that second, with respect to the square meter boxes that are shaded as compared to the ones that are not. A good approach for analyzing turbine shadow impact for clear days is to use the clear sky equations[4], which are also shown in Appendix A

(Steps 1 to 11). The equations help to compute the intensity of the beam, diffuse, and ground reflection components when there is a bright sun. To determine the position of the sun and the beam component on a panel surface, we use equations in Appendix B (Steps 12 through 20). These equations were programmed in Matlab[7] where the shadow cast by the tower and the blades for each second were projected onto the selected land plot, excluding the 100 m diameter maintenance pad. For each second, if the shadow fell on the cell, the PV in that cell would receive only the diffuse and ground reflection components, shown in steps 9 and 10, on their plane of array as computed by the Clear Sky equations. If the shadow did not fall on the cell, then the PV in that cell would receive the full incident solar energy, calculated in step 11. Thus we have two calculated values for $P_{incident}$ for each second, one for the shaded regions from the shadow of the turbine and the other for the regions that have no shadows, using the clear sky equations. At the end of the day, the solar energy for each second of data is added for each cell on the grid to obtain the daily solar kWh harvest.

4.3 METHOD 2. PREDICTED IMPACT USING ACTUAL SOLAR RADIATION MEASUREMENTS

Turbine shadow impact is less on cloudy days because there are already cloud shadows on the ground and the beam of the sun is less intense on average. When actual global horizontal (GH) and diffuse horizontal (DH) measurements are available, we first compute the sun's position using Steps 12 through 20[13]. Then, we compute the incident solar energy on a panel surface – in a cell, using the GH and DH values available to us for the specific second, according to the following:

- If the turbine shadow (see Figure A4 in the Appendix) does not fall on a one square meter study cell, then we use GH and DH with equation (1) to predict the incident solar energy on that cell,

$$P_{incident} = DH + \frac{(GH - DH)}{\cos\left(\theta_{sun}^{zenith}\right)} \cdot \cos\left(\beta_{incident}\right) \quad (1)$$

- If the turbine shadow does fall on the study cell, then the incident solar energy on the cell is equal to only the DH component.

As mentioned previously, the four study days are the two equinoxes, and the two solstices. So as to not bias the findings with one particular unusual day, we chose a seven-day consecutive period for each of the four days, thus achieving some averaging of the actual data. An important point to note about the data used is that the data obtained was given as 5-minute data. To adjust the data and use it per second basis, the data was linearly fit to obtain 1-second data. The results from both methods 1 and 2 are shown in section 5. But before that, it is important to understand the different implementations of the shading from the wind turbine.

4.4 SHADING IMPLEMENTATIONS

The shadows projected from a wind turbine have been modeled in two different ways. These are as follows:

1. The tower is considered to be a single line of a specific tip-top height. Where, the tip top height is the maximum height from the base of the turbine to the tip of the blade at its highest point. As mentioned earlier this value has been assumed to be 120 m in all the calculations. This is the best-case scenario, where the shading from the wind turbine is considered to be minimum, as the blades of the wind

turbine are facing a direction 90° from the direction of the sun. In this case, the blades project a shadow that is very narrow; hence we consider it as a line.

2. In the second case, the tower is considered to be a single line, only till the hub height, which is the location where the center of the blades is attached to the wind turbine mast. This height in the calculations is assumed to be 80 m. In this case, we assume that the blades are directly facing the sun, and hence produce a fast moving elliptical shadow. Even though the shadow is not a complete ellipse, because of the high speed of the blades, we consider the shadow from the blades to be a complete ellipse. Here, the width of the elliptical shadow stays constant and is equal to the diameter of the blades, and the length of the shadow is found using the same method shown in Figure A4 in the Appendix. The angle of rotation of the ellipse is equal to the angle of the shadow azimuth.

An important aspect of the simulations of both these implementations in Matlab is that the grids plotted are created using matrices. Since we use matrices, the axis values increase from 1,1 to 1000,1000 for a plot area of 1 km^2 or 1000 m by 1000 m grid. Due to this we will see that when the wind turbine is placed in the center of a grid layout of area 1 km^2, its position is 500,500 instead of what might be expected (being places at the origin at 0,0).

Chapter 5

Results and Analysis

5.1 One Turbine on a 1 km^2 Plot with Shading Implementation 1

In the first set of simulations that were run, a plot size of 1000 m by 1000 m was used. The wind turbine in this case is located at the center of the plot (500,500). In order to get maximum resolution, Figures 5 to 8 (a and b) show a zoomed view of the grid from axis values 200 to 800. In this set of simulations, we have used the first implementation of the shading effect, where we show the minimum shading using the best-case scenario. These simulations are run using both the "Clear Sky Equations" and the "Actual Solar Radiation Measurements".

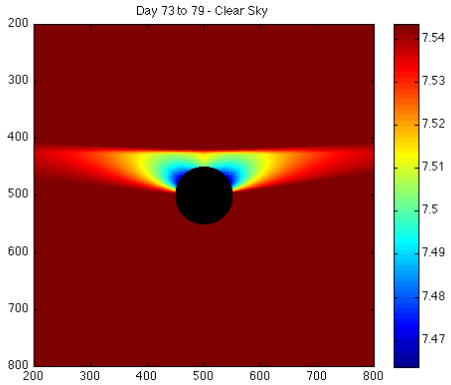

Fig 5a – Spring Equinox, Clear Sky, Incident Daily Solar kWh

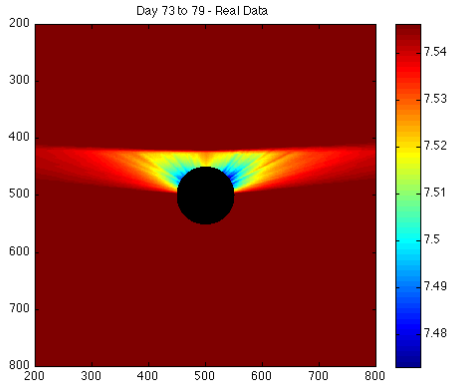

Fig 5b – Spring Equinox, Real Data, Incident Daily Solar kWh

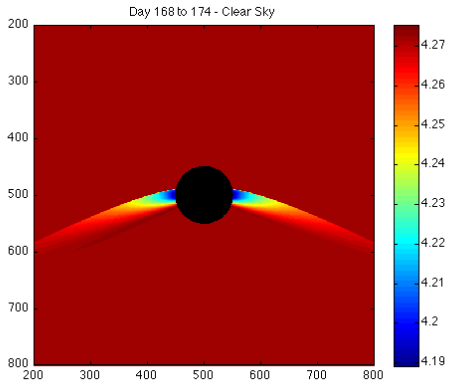

Fig 6a – Summer Solstice, Clear Sky, Incident Daily Solar kWh

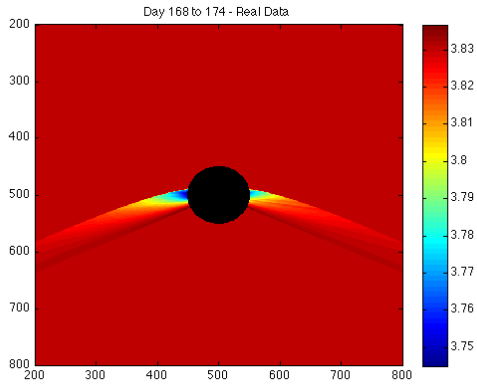

Fig 6b – Summer Solstice, Real Data, Incident Daily Solar kWh

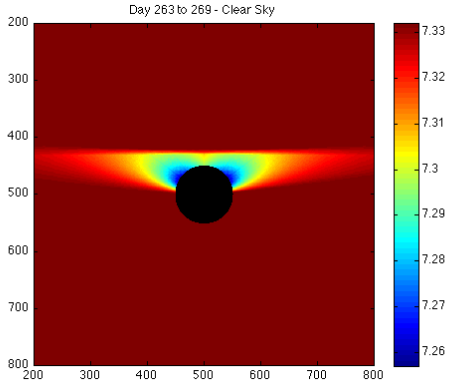

Fig 7a – Fall Equinox, Clear Sky, Incident Daily Solar kWh

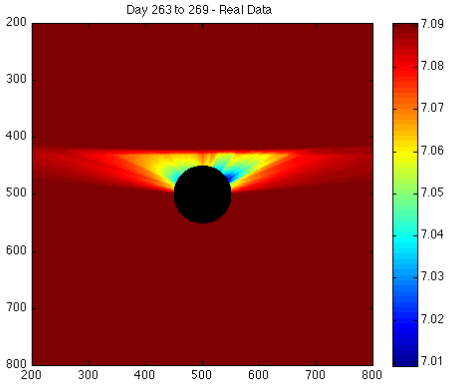

Fig 7b – Fall Equinox, Real Data, Incident Daily Solar kWh

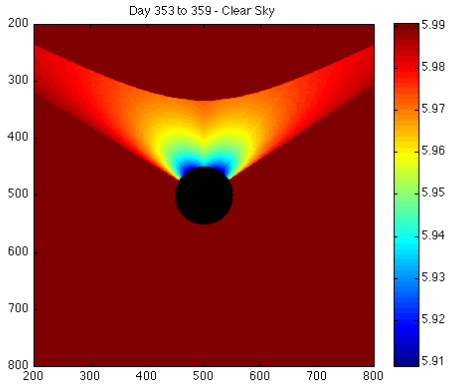

Fig 8a – Winter Solstice, Clear Sky, Incident Daily Solar kWh

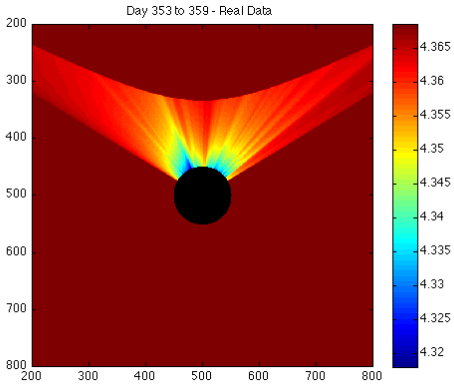

Fig 8b – Winter Solstice, Real Data, Incident Daily Solar kWh

In Figures 5 to 8 above, it can be easily seen that the maximum reduction in the incident daily solar kWh for any set of days is only 1-2%, which is really small. Also the black circle at the center of the plots indicates the turbine maintenance pad, where nothing can be placed. Hence, we do not make solar harvest measurements for that region. Subsequently, most of the maximum reduction of 1-2% in the daily solar kWh occurs in the region closest to the pad for all the cases shown in the figures. An important point to note is that the positive Y-axis corresponds to North in Figures 5 to 8.

One thing that is clearly visible from Figures 5 to 8 is the variation in the difference between the graphs obtained using by using the “Clear Sky Equations” and the “Actual Solar Radiation Measurements”. Depending on which data set we look at, there

is either a 10% difference or no difference at all, in the daily solar kWh between the two measurements. This difference can be attributed to the daily cloud movements. To understand this, lets look at the Actual GH measurements that were used for both these cases, in Figures 9 and 10. The value for the X-axis (not shown) corresponds to the times from sunrise to sunset for each of the 7-day periods.

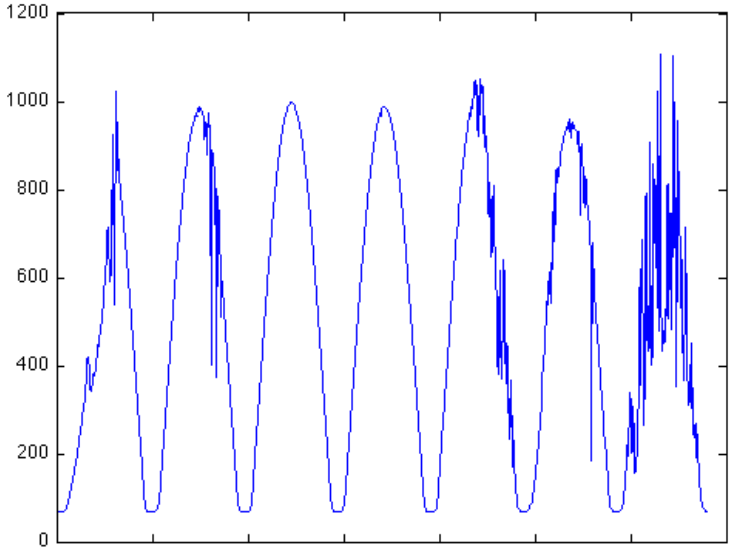

Figure 9 – Spring Equinox, days 73 to 79, Actual GH measurements in units of W/m^2

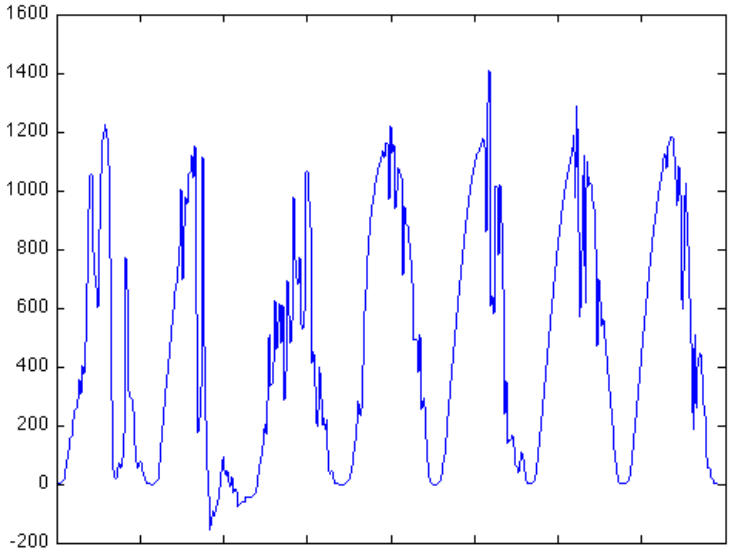

Figure 10 – Summer Solstice, days 168 to 174, Actual GH measurements in units of W/m^2

For example, looking at the spring equinox data in Figures 5a and 5b, it is pretty obvious that clouds in the sky did not significantly reduce the GH measurements on those days. Looking at Figure 9 validates this theory. Similarly, when we look at the summer solstice data in Figures 6a and 6b, it seems like there must have been a lot of cloud movement that caused a significant reduction in available solar radiation or GH. Looking at Figure 10, where it is seen that there was significant cloud movement almost everyday of the week, proves this as well.

Next, we take a look at the effect that the shadows from neighboring wind turbines may have on the total solar harvest.

5.2 NINE TURBINES ON A 900M X 3000M PLOT WITH SHADING IMPLEMENTATION 1

In the second set of simulations that were run, a plot size of 900 m by 3000 m was used. There were 9 wind turbines used in this case. These were located at the following positions – Turbine 1 at (500,150), Turbine 2 at (500,450), Turbine 3 at (500,750), Turbine 4 at (1500,150), Turbine 5 at (1500,450), Turbine 6 at (1500,750), Turbine 7 at (2500,150), Turbine 8 at (2500,450), and Turbine 9 at (2500,750). The positions of these turbines were determined based on the required size per wind turbine, as shown in Figure A3. Nine wind turbines were chosen for this simulation to exhaustively show all scenarios possible for the overlapping shadows from different neighboring turbines. In this set of simulations, we have again used the first implementation of the shading effect, where we show the minimum shading using the best-case scenario. Theses simulations are run using both the "Clear Sky Equations" and the "Actual Solar Radiation Measurements". Again, the positive Y-axis corresponds to the geographical North in Figures 11 to 14.

In Figures 11 to 14, on the following pages, the most important result obtained is that for most study days of the year, there is not much of a shadow overlap from neighboring wind turbine shadows. But in Figures 14a and 14b, we can see quite a dominant overlap of shadows. Even though the shadows from different turbines intersect at multiple places in the plot area for the winter solstice simulations, the reduction in the daily solar kWh harvest is not significant enough to worry about it. In the areas where the shadows from different turbines overlap, the overlapping shading effect causes reduction of the daily solar kWh harvest by 0.2%, which is very small. This shows that we never have to worry about the overall reduction in daily solar kWh harvest due to the shading from neighboring wind turbines.

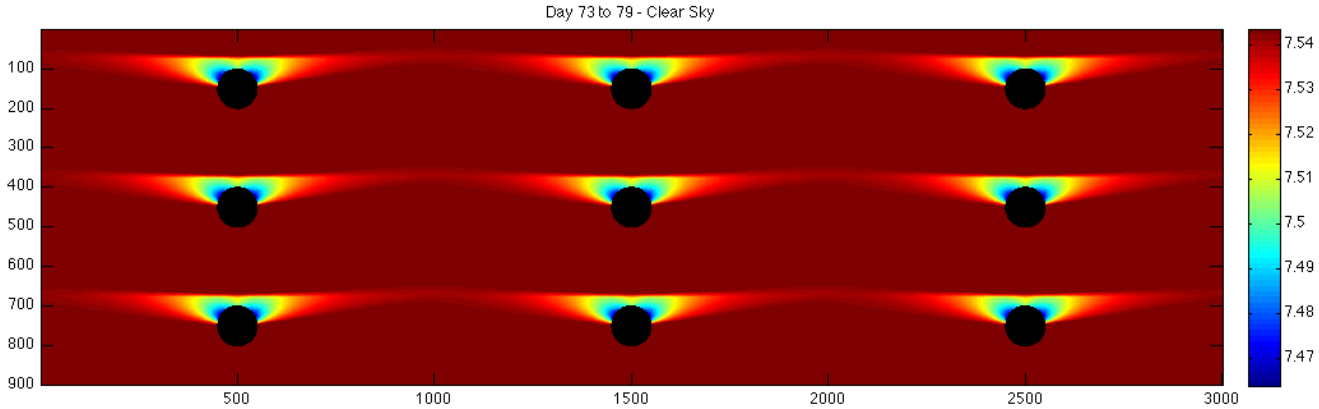

Figure 11a – Spring Equinox, Clear Sky, Incident Daily Solar kWh for a plot with nine wind turbines

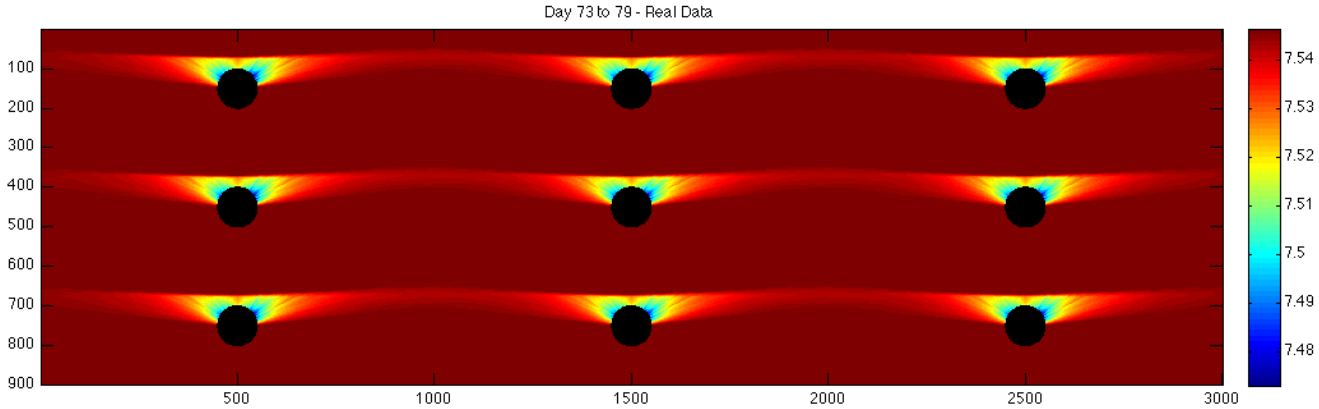

Figure 11b – Spring Equinox, Real Data, Incident Daily Solar kWh for a plot with nine wind turbines

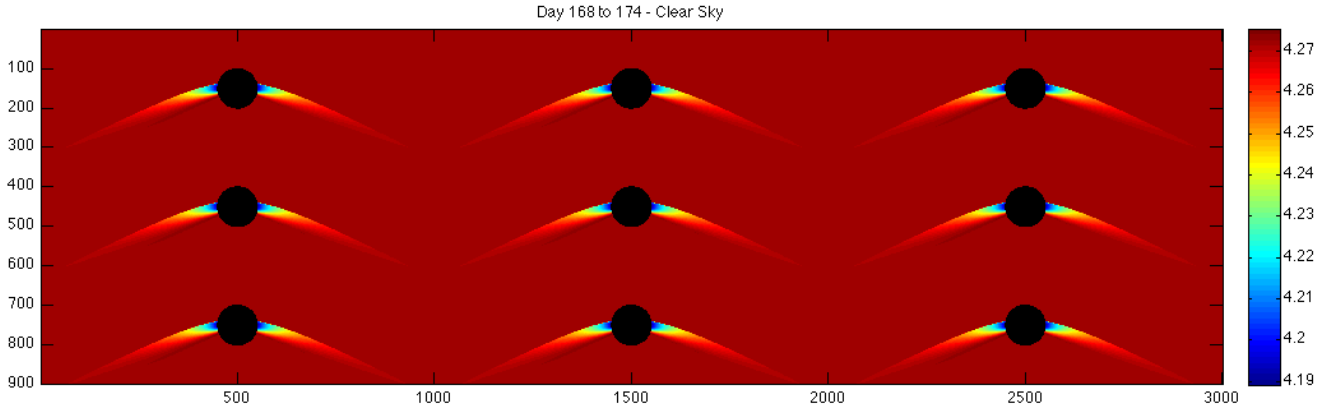

Figure 12a – Summer Solstice, Clear Sky, Incident Daily Solar kWh for a plot with nine wind turbines

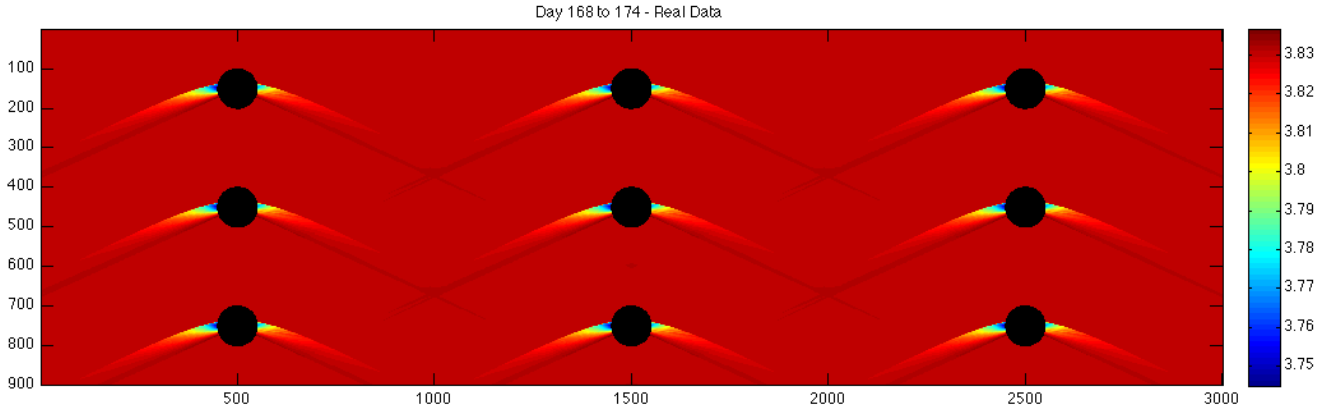

Figure 12b – Summer Solstice, Real Data, Incident Daily Solar kWh for a plot with nine wind turbines

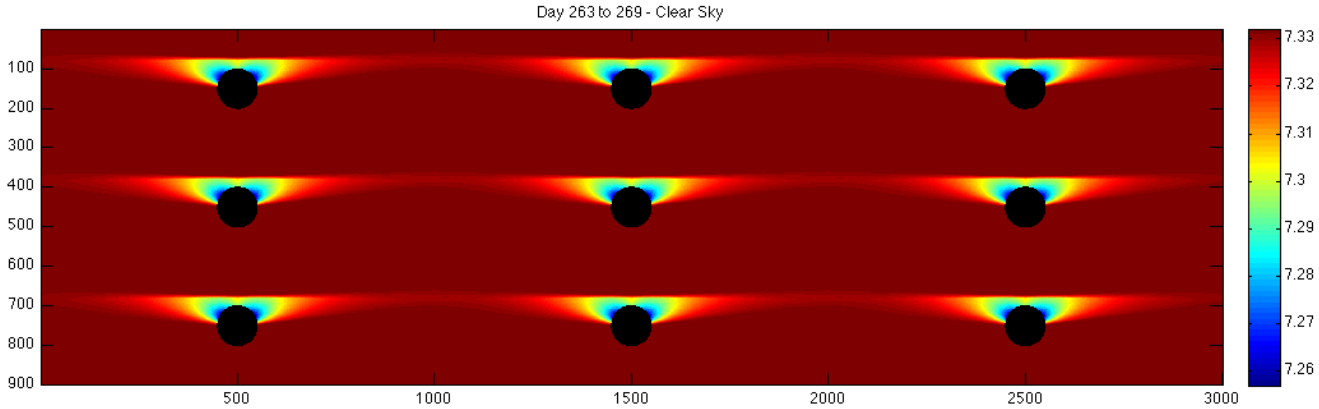

Figure 13a – Fall Equinox, Clear Sky, Incident Daily Solar kWh for a plot with nine wind turbines

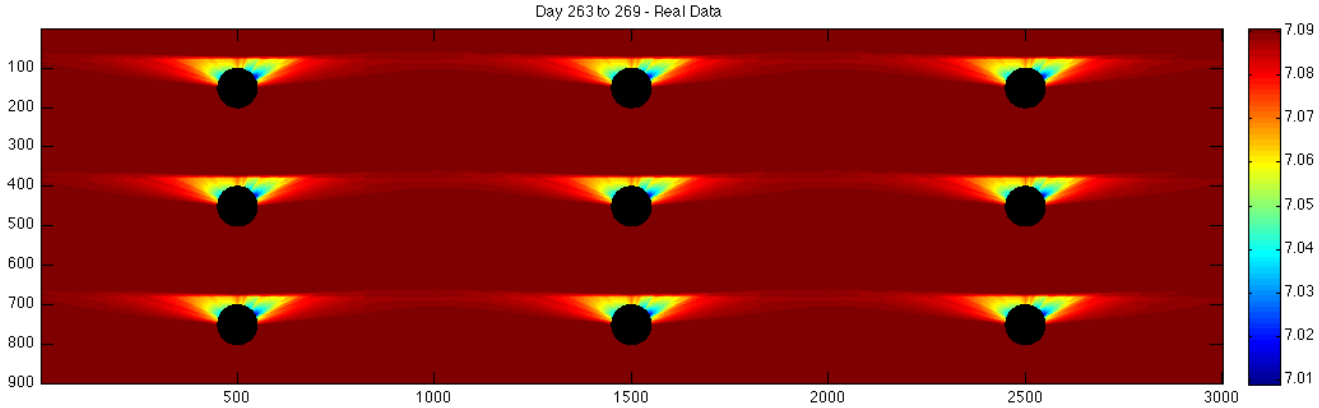

Figure 13b – Fall Equinox, Real Data, Incident Daily Solar kWh for a plot with nine wind turbines

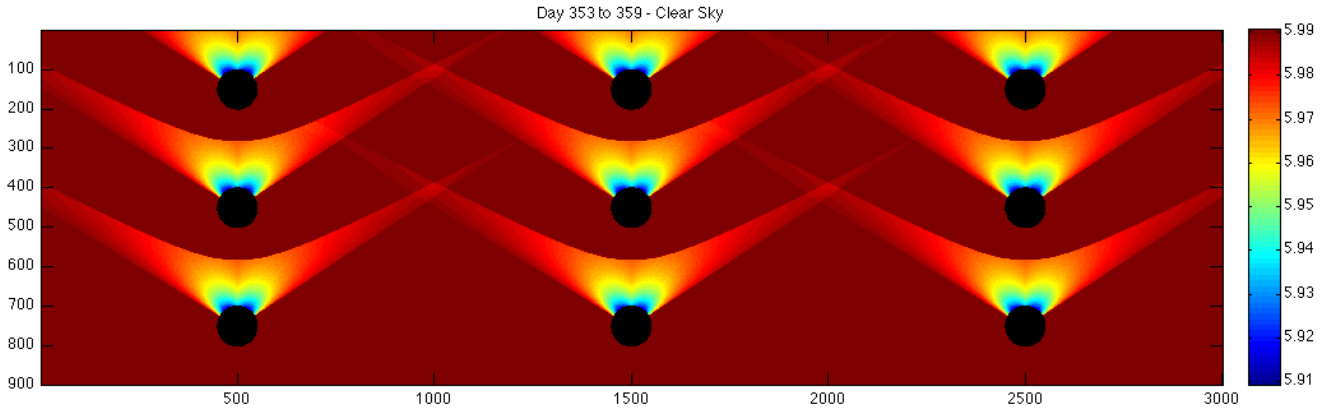

Figure 14a – Winter Solstice, Clear Sky, Incident Daily Solar kWh for a plot with nine wind turbines

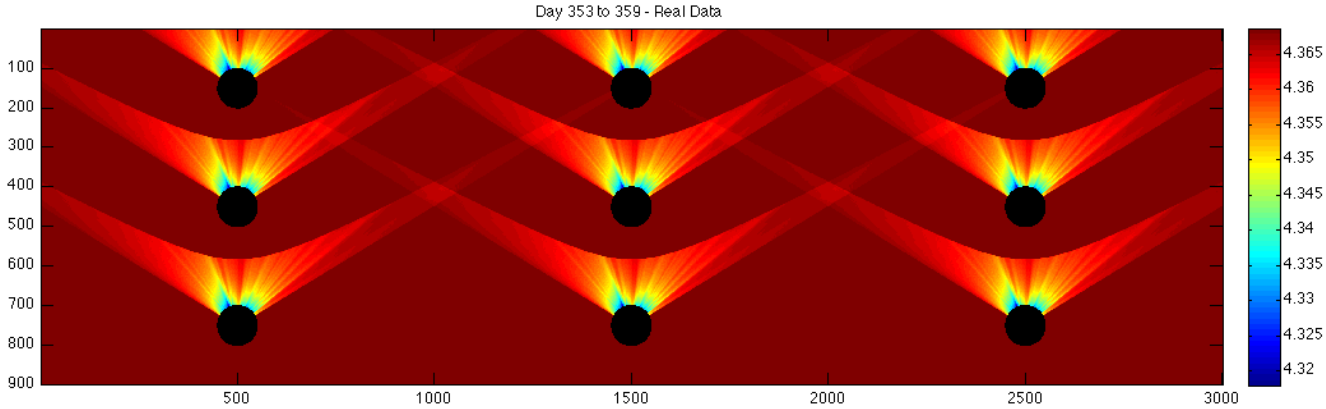

Figure 14b – Winter Solstice, Real Data, Incident Daily Solar kWh for a plot with nine wind turbines

5.3 ONE TURBINE ON A 1 KM^2 PLOT WITH SHADING IMPLEMENTATION 2

In the third set of simulations that were run, a plot size of 1000 m by 1000 m was used, similar to the first set. The wind turbine in this case is also located at the center of the plot at (500,500). In Figures 15 to 18, we view the entire plot area because in these figures the magnitude of reduction in the daily solar kWh is much higher and hence, more significant. In this set of simulations, we have used the second implementation of the shading effect, where we show the maximum shading possible using the worst-case scenario for the overall daily solar kWh. Theses simulations are run using only the "Clear Sky Equations". And as before, it is important to note that the positive Y-axis corresponds to the geographical North in Figures 15 to 18, and that the turbine maintenance pads are shown as the black circles.

Here, the shading implementation 2 is only run with a single turbine on the 1 km^2 plot area, because we saw that the maximum shading that occurs affects only the immediate area surrounding the wind turbine. Although, there are areas where shadows from multiple turbines overlap, as seen in section 5.2, the reduction in the daily solar kWh due to those shadows is not significant (less than 0.2%). This was clearly visible in Figures 11 to 14, and can be negated in this simulation set. Thus, we want to focus on the total land plot and see how much of the land area is rendered useless for solar generation purposes due to the shading from the turbine, in this worst-case shading scenario.

Looking at Figures 15 to 18, we can say that even though the overall reduction in daily solar kWh is significantly higher in these cases, the maximum losses are still located very close to the maintenance pad, as was seen in the previous simulation sets. In Figures 15 through 18, the maximum loss in daily solar kWh is between 32% and 37% for the four sets of days. Out of the days under consideration, the most significant

shading effect occurs during the winter solstice with a maximum loss of 37%. During the winter solstice most of the losses are within a distance of approximately 150 m, perpendicularly away from the position of the turbine.

Given all these scenarios, let us consider another circular area of radius 50 m, centered at a distance of 100 m North from the position of the wind turbine. Now, we encompass the two circular pads with a rectangle, such that the rectangular area would contain the two circular areas falling within it, as shown in the appendix in Figure A5.

Looking at Figure A5, it is evident that we would only leave out an area of 20,000 m^2 out of a total area of 300,000 m^2, due to the extreme shading conditions from the shading implementation 2 (worst-case scenario shading). This still leaves a pretty large area, approximately 93% of the total area of the wind turbine plot empty for use with solar panels. Although, even this part of the remaining plot has some losses, the losses here are significantly smaller.

The Figures 15 through 18, which have been discussed here, are on the pages that follow.

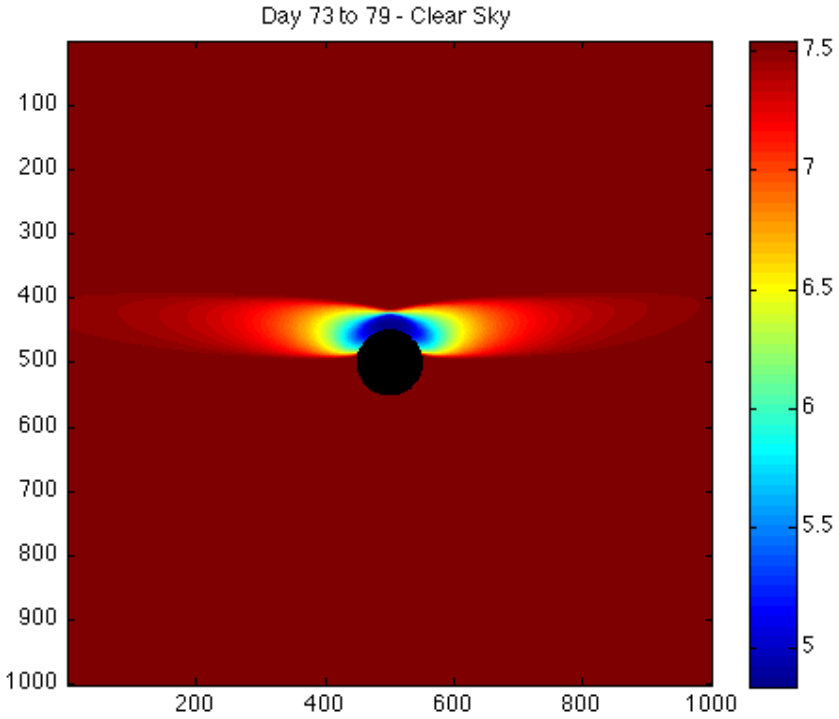

Figure 15 – Spring Equinox, Clear Sky, Incident Daily Solar kWh for a plot with one wind turbine using Shading Implementation 2

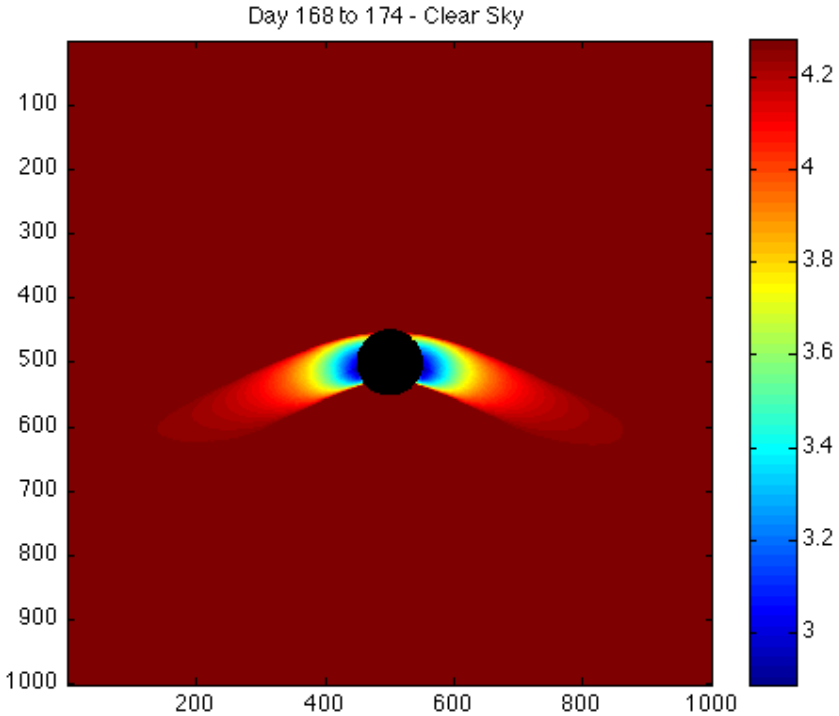

Figure 16 – Summer Solstice, Clear Sky, Incident Daily Solar kWh for a plot with one wind turbine using Shading Implementation 2

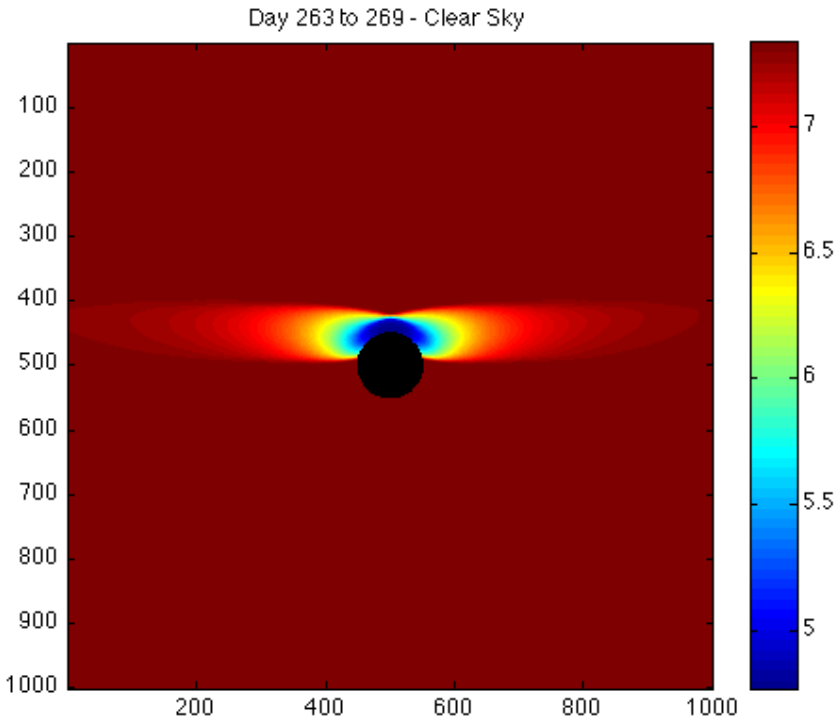

Figure 17 – Fall Equinox, Clear Sky, Incident Daily Solar kWh for a plot with one wind turbine using Shading Implementation 2

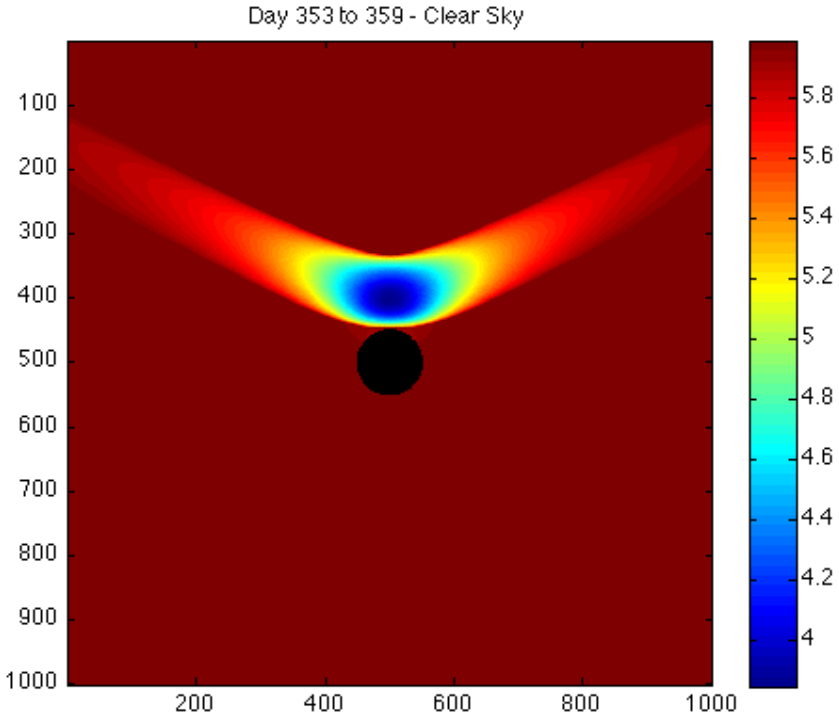

Figure 18 – Winter Solstice, Clear Sky, Incident Daily Solar kWh for a plot with one wind turbine using Shading Implementation 2

5.4 NINE TURBINES ON A 900M X 3000M PLOT WITH SHADING IMPLEMENTATION 1, FOR VARYING PREVAILING WIND DIRECTIONS FOR WINTER SOLSTICE

In the fourth simulation set, we take prevailing wind directions into consideration. Wind power plants usually have the wind turbines setup in a pattern based on the regular prevailing wind direction. For simplicity, all of the figures showing multiple wind turbines in Figures 11 through 14 are shown to be setup for prevailing wind in the East-West direction.

Now, we consider two more wind direction orientations to see if the shading profile changes significantly for the different prevailing wind directions. The two prevailing wind directions chosen for analyzing in this section are North-South direction and NorthWest-SouthEast direction. These are shown in Figures 19 and 20, respectively. The North-South direction case is shown to easily explain how the change in prevailing wind direction can change the setup of a wind power plant. The NorthWest-SouthEast direction is shown, as that is the most common prevailing wind direction in West Texas. It should be noted that when a prevailing wind direction is mentioned, for example East-West, the simulations are applicable for prevailing winds flowing from East to West and also for prevailing winds from West to East. For this set of simulations we use only the winter solstice 7-day period, as it was seen in all the earlier simulations that the winter solstice days had the maximum shading.

To properly understand the change that occurs in Figures 19 and 20, it should be noted that the effective axis corresponding to the geographical North changes in them. For Figure 19, the +X axis corresponds to the geographical North, instead of the +Y axis corresponding to North as was seen in all the Figures from 5 to 18 (excluding Figures 9 and 10, which show the GH measurements and not the daily solar kWh).

Although, in Figures 19 and 20 it is seen that the shading profile and the overlapping shadow positions change a little, the overall reduction in daily solar kWh per m^2 does not change. Also, the bounds of the daily solar kWh stay exactly the same as was seen in Figure 14b.

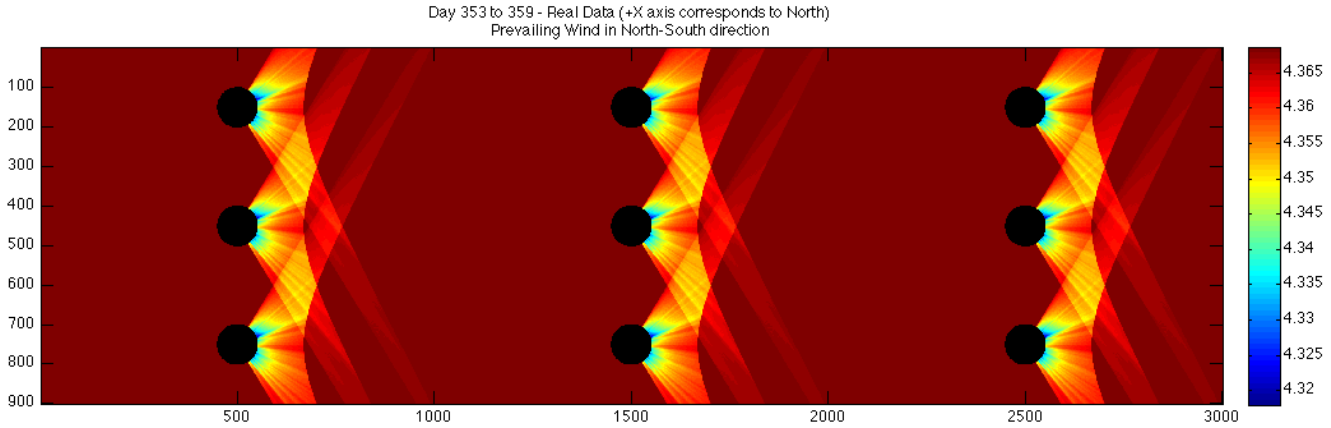

Figure 19 – Winter Solstice, Real Data, Incident Daily Solar kWh for a plot with nine wind turbines with the Prevailing Wind in the North-South direction

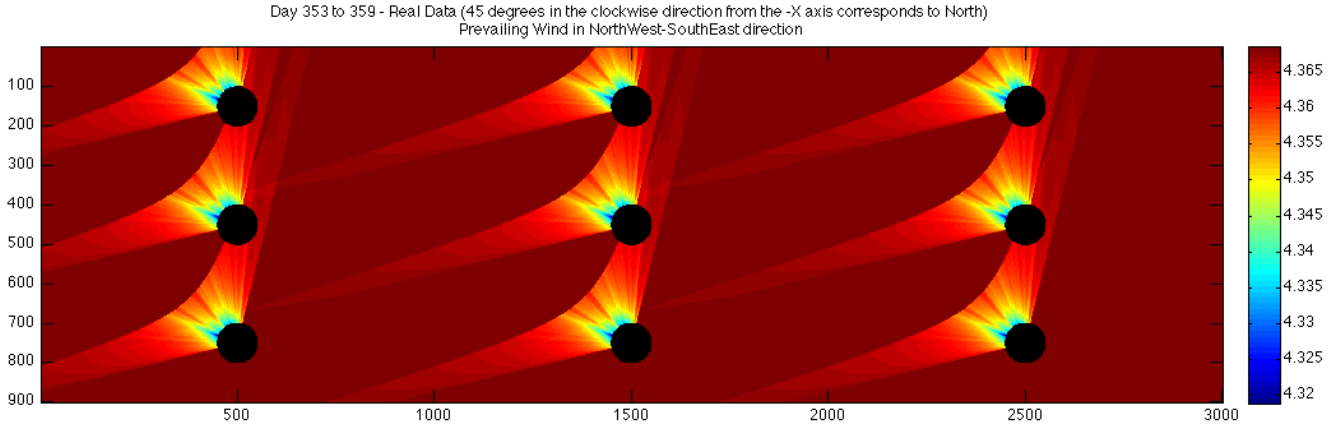

Figure 20 – Winter Solstice, Real Data, Incident Daily Solar kWh for a plot with nine wind turbines with the Prevailing Wind in the NorthWest-SouthEast direction

Chapter 6

Conclusion

As can be seen from Figures 5 through 18 (excluding Figures 9 and 10, which show the GH measurements and not the daily solar kWh), which have been obtained from the simulations – the overall area of the wind power plant that is affected by the shading from the wind turbines is very small and is only concentrated in the immediate vicinity of the wind turbines, in shading implementation 1. This implementation also has a very small reduction in the daily solar kWh of only about 1-2%.

In shading implementation 2, the area that is affected by the shading is larger and furthermore, the effect of the shading causes the daily solar kWh to reduce more significantly. In the cases shown in Figures 15 to 18, the maximum reduction in the daily kWh is found to be approximately 37%. In the analysis, I mentioned that we could quite easily reserve an area of 20,000 m^2 as shown in the Appendix Figure A5, where we would not place any solar panels. This would still leave us with almost 93% of the wind turbine plot to utilize for setting up solar panels. This would help generate electricity during times of high solar potential and low wind potential by utilizing the pre-allocated land resources and electrical infrastructure to the maximum potential. This also helps in bringing down the overall initial capital investment per MW.

One point to take note of, is the fact that the overall shading occurring on a wind power plant is a combination of shading implementations 1 and 2. Most of the time during the day the wind turbine blades are facing in the direction of the prevailing wind. Thus the amount of time during the day when the shading occurs due to shading implementation 2 is very small, probably in the order of an hour at most. Thus, the

effective reduction in daily solar kWh would be minimal. This results in creating a huge cost benefit and opportunity for creating integrated Wind and Solar Power Plants.

Appendices

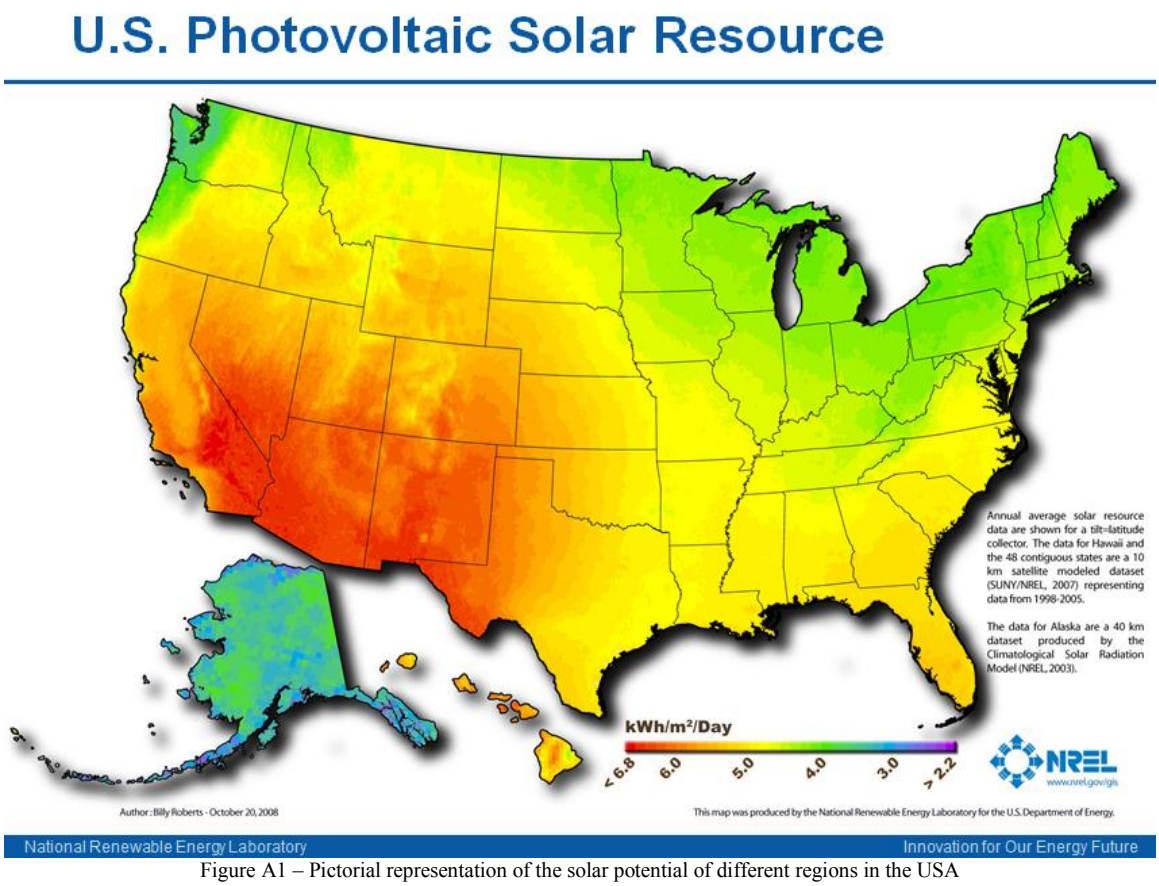

Figure A1 – Pictorial representation of the solar potential of different regions in the USA

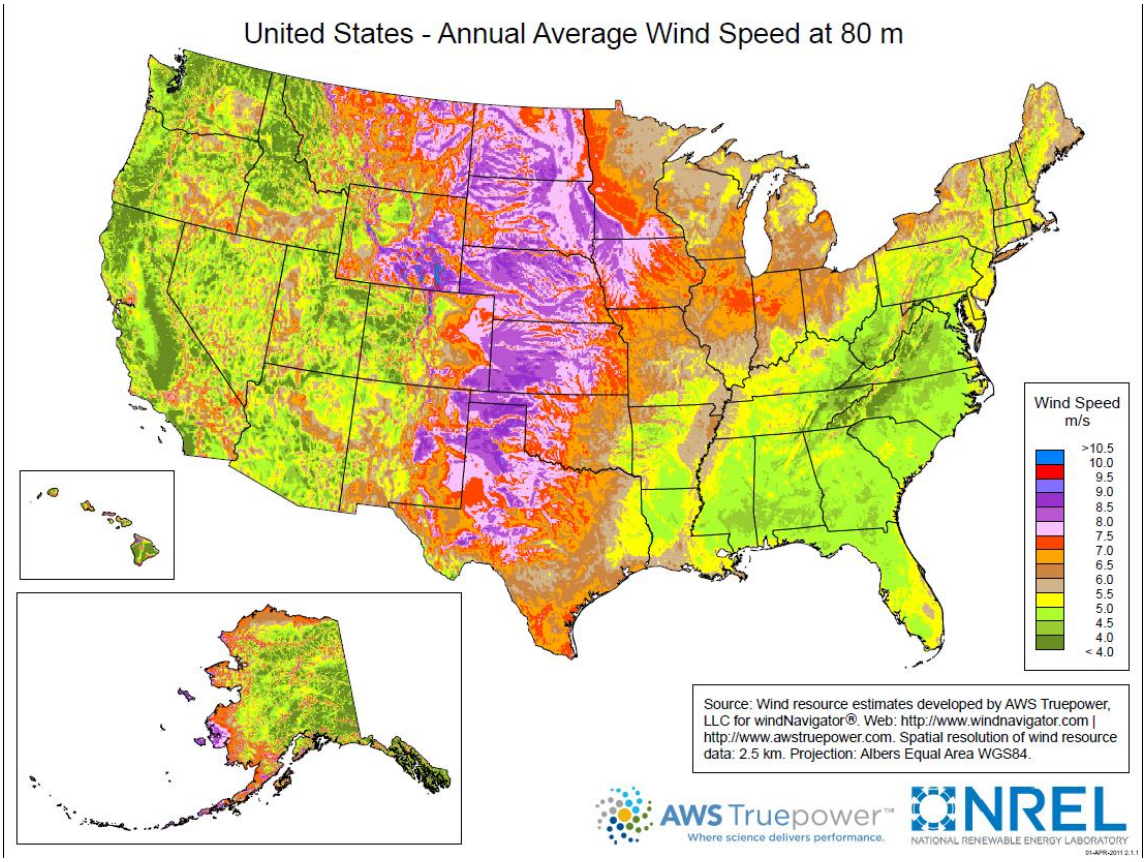

Figure A2 – Pictorial representation of the wind potential of different regions in the USA

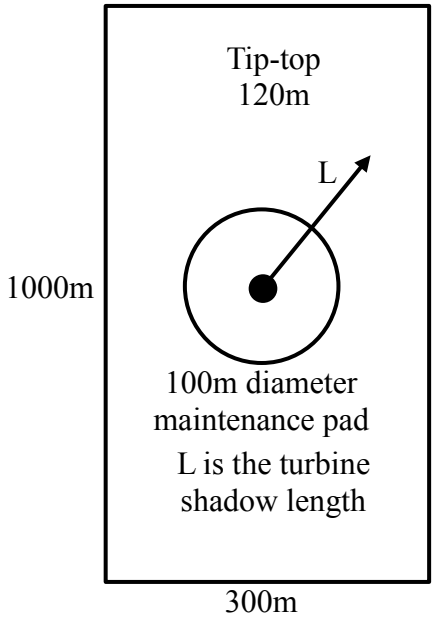

Figure A3– Diagram showing the plot of land dedicated to each wind turbine

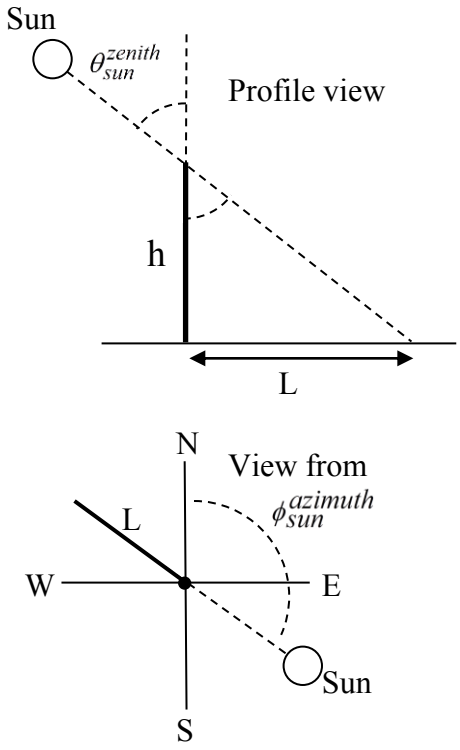

Shadow length L $= h \bullet \tan(\theta_{sun}^{zenith})$

Shadow azimuth = $\phi_{sun}^{azimuth} + 180°$

Figure A4. Geometry to compute shadow length and azimuth of tower tip-top height

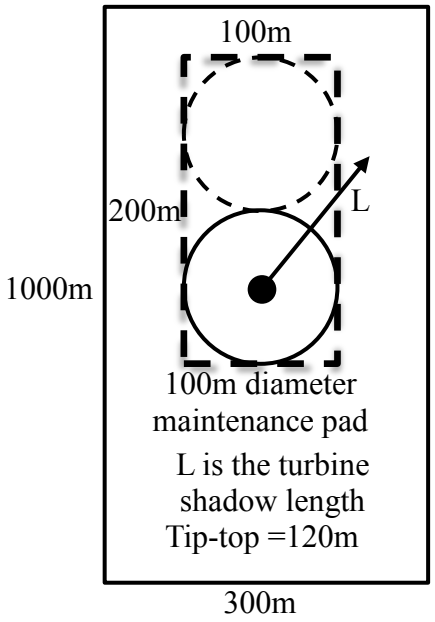

Figure A5– Diagram showing the plot of land dedicated to each wind turbine and its shadow based on the worst case scenario

A. CLEAR SKY EQUATIONS

Step 1. Air Mass Ratio m (relative atmosphere travel distance to reach Earth's surface)

$$m = \frac{1}{\cos(\theta_{zenith}^{sun})}$$

Step 2. Apparent Extraterrestrial Flux A

$$A = 1160 + 75 \bullet \sin\left[\frac{360}{365}(n - 275)\right] \text{ W/m}^2$$

Step 3. Optical Depth k

$$k = 0.174 + 0.035 \bullet \sin\left[\frac{360}{365}(n - 100)\right]$$

Step 4. Beam Reaching Earth I_B

$$I_B = Ae^{-km} \text{ W/m}^2$$

Step 5. Sky Diffuse Factor C

$$C = 0.095 + 0.04 \bullet \sin\left[\frac{360}{365}(n - 100)\right]$$

Step 6. Diffuse Radiation on Horizontal Surface I_{DH}

$$I_{DH} = C \bullet I_B \text{ W/m}^2$$

Step 7. Beam Normal to a Panel I_{BC}

$$I_{BC} = I_B \bullet \cos(\beta_{incident}) \text{ W/m}^2$$

Step 8. Beam on Horizontal Surface I_{BH}

$$I_{BH} = I_B \bullet \cos(\theta_{zenith}^{sun}) \text{ W/m}^2$$

Step 9. Diffuse Radiation on Panel I_{DC}

$$I_{DC} = I_{DH}\left(\frac{1+\cos\theta_{tilt}^{panel}}{2}\right) \text{ W/m}^2$$

Step 10. Reflected Radiation Panel I_{RC} (from the ground and surrounding objects)

$$I_{RC} = \rho \bullet (I_{BH} + I_{DH}) \bullet \left(\frac{1-\cos\theta_{tilt}^{panel}}{2}\right) \text{ W/m}^2,$$

where ground reflectance ρ is typically 0.2, but can be as large as 0.8 for fresh snow.

Step 11. Total Clear Sky Insolation on Panel I_C

$$I_C = I_{BC} + I_{DC} + I_{RC} \text{ W/m}^2$$

B. SUN POSITION EQUATIONS

Step 12. Sun declination angle, δ (in degrees)

$\delta = 23.45\sin(B)$, where

$B = \frac{360}{365}(n-81)$ degrees , and

n = day of year (i.e., 1,2,3, … , 364,365).

Step 13. Equation of time, E_{qt} (in decimal minutes)

$$E_{qt} = 9.87\sin(2B) - 7.53\cos(B) - 1.5\sin(B)$$

Step 14. Solar time, T_{solar} (in decimal hours)

$$T_{solar} = T_{local} + \frac{E_{qt}}{60} + \frac{(Long_{timezone} - Long_{local})}{15}$$

where

- T_{local} is local standard time in decimal hours,
- $Long_{timezone}$ is the longitude at the eastern edge of the time zone (e.g., $90°$ for Central Standard Time).

  $(Long_{timezone} - Long_{local})$ is entered as "Longitude shift (deg)."

Step 15. Hour angle, H (in degrees)

$$H = 15 \bullet (12 - T_{solar})$$

Step 16. Cosine of the zenith angle, θ_{sun}^{zenith} (in degrees)

$$\cos\left(\theta_{sun}^{zenith}\right) = \sin(L)\sin(\delta) + \cos(L)\cos(\delta)\cos(H)$$

where L is the latitude of the location.

Solar azimuth comes from the calculations in Step 17 and 18. Using the formulas for solar radiation on tilted surfaces, consider vertical surfaces directed east and south:

Step 17. The fraction of direct component of solar radiation on an east-facing vertical surface is

$$f_{VE} = \cos(\delta)\sin(H)$$

Step 18. The fraction of direct component of solar radiation on a south-facing vertical surface is

$$f_{VS} = -\sin(\delta)\cos(L) + \cos(\delta)\sin(L)\cos(H)$$

Steps 17 and 18 correspond to the projections on east and south facing vertical planes. Given those, the sun's azimuth angle $\phi_{sun}^{azimuth}$ can be found as follows:

Step 19. Sun's azimuth angle, $\phi_{sun}^{azimuth}$ (in degrees)

If $f_{VE} \geq 0$, $\phi_{sun}^{azimuth} = \cos^{-1}\left(\frac{-f_{VS}}{\sqrt{f_{VE}^2 + f_{VS}^2}}\right)$ degrees,

If $f_{VE} < 0$, $f_{sun}^{azimuth} = 180 + \cos^{-1}\left(\frac{f_{VS}}{\sqrt{f_{VE}^2 + f_{VS}^2}}\right)$

Step 20. Cosine of the Incident angle, β (in degrees)

$$\cos\beta_{incident} = \sin\theta_{sun}^{zenith}\sin\theta_{panel}^{tilt}\cos\left(\phi_{sun}^{azimuth} - \phi_{panel}^{azimuth}\right) + \cos\theta_{sun}^{zenith}\cos\theta_{panel}^{tilt}$$

References

1) “2010 U.S. Wind Industry Annual Market Report: Rankings”, *American Wind Energy Association*, May. 2011. Web. 12 Nov. 2011.
Web.<http://www.awea.org/learnabout/publications/factsheets/upload/2010-Annual-Market-Report-Rankings-Fact-Sheet-May-2011.pdf>.

2) "Electric Power Annual Statistics", *U.S. Energy Information Administration*, n.d. Web. 17 Nov. 2011.
Web. <http://www.eia.gov/electricity/annual/pdf/tablees1.pdf>.

3) "Fact Sheet", *Puget Sound Energy*, n.d. Web. 5 Oct. 2011.
Web.<http://www.pse.com/aboutpse/PseNewsroom/MediaKit/057_Wild_Horse_English.pdf>.

4) G. M. Masters, *The Solar Resource.*
Renewable and Efficient Electric Power Systems
John Wiley & Sons, 2004.

5) Gronewold, Nathaniel, "One quarter of the world lacks electricity", *Scientific American*, 24 Nov. 2009. Web. 13 Oct. 2011.
Web.<http://www.scientificamerican.com/article.cfm?id=electricity-gap-developing-countries-energy-wood-charcoal>.

6) Jahdi, Saeed ; Loi Lei Lai ; Nankoo, Daniel, “Grid Integration of Wind-Solar Hybrid Renewables Using AC/DC Converters as DG Power Sources”, *Sustainable Technologies (WCST), 2011 World Congress on*, 7-10 Nov. 2011.

7) Matlab & Simulink Student Version, MathWorks, 2011.

8) Morgan, Jason, "Comparing Energy Costs of Nuclear, Coal, Gas, Wind, and Solar", *Nuclear Fissionary*, 2 Apr. 2010. Web. 17 Sep. 2011.
Web. <http://nuclearfissionary.com/2010/04/02/comparing-energy-costs-of-nuclear-coal-gas-wind-and-solar/>.

9) "Renewables 2011: Global status report", *REN21*, n.d. Web. 7 Oct. 2011.
Web. <http://www.ren21.net/Portals/97/documents/GSR/REN21_GSR2011.pdf>.

10) "Renewable Energy Technology Resource Maps for the United States", *National Renewable Energy Laboratory*, Aug. 2009. Web. 24 Sep. 2011.
Web. <http://www.nrel.gov/gis/docs/resource_maps_200905.ppt>.

11) Sandru, Ovidiu, "1 MW Solar-Powered Parking Lot Opening in Bordentown, NJ", *The Green Optimistic*, 15 Jan. 2010. Web. 27 Sep. 2011.
Web.<http://www.greenoptimistic.com/2010/01/15/1-mw-solar-powered-parking-lot-opening-in-bordentown-nj/>.

12) "U.S. Electric Net Summer Capacity", *U. S. Energy Information Administration*, Aug. 2010. Web. 10 Oct. 2011.
Web. <http://www.eia.gov/cneaf/alternate/page/renew_energy_consump/table4.html>.

13) W. Mack Grady, Power Electronics, EE 462L Lecture Notes, http://users.ece.utexas.edu/~grady/courses.html

Vita

The author of this thesis, Sahil Shanghavi, was born and raised in Calcutta, India. After finishing his high school education there, he moved to the United States of America to avail of the different opportunities available, and pursue his education in the field of engineering. He graduated with Suma Cum Laude honors with a Bachelors of Science in Electrical Engineering and a minor in Engineering Management at the University of Massachusetts at Amherst in 2010. He earned the Dean's List distinction in each of the semesters he was enrolled there. He also won the University's coveted 21st Century Leader Award his graduating semester.

His interest in Renewable Energy started with his honors capstone project, during his senior year. For his project, he had the opportunity to setup a 400 Watt wind turbine on top of one of the engineering buildings. This led to him joining the University of Texas at Austin to pursue a Masters degree in Electrical Engineering with a concentration in Energy Systems.

He plans to gain some valuable work experience in the years following his graduation from UT Austin, in the field of Power and Energy. After gaining some industry experience he hopes to help out with rural electrification efforts throughout the world, starting with his home country of India.

Email : sahil.shanghavi@gmail.com

This thesis was typed by Sahil Shanghavi.